IEEE Access
Multidisciplinary ⋮ Rapid Review ⋮ Open Access Journal

Received August 24, 2021, accepted September 7, 2021, date of publication September 17, 2021,
date of current version September 29, 2021.

Digital Object Identifier 10.1109/ACCESS.2021.3113695

Impact of the Link Length on the Delay in Two-Way Signal Coordination

YANLEI CUI[1], YI YU[1], AND DIANHAI WANG[1,2,3]
[1]College of Civil Engineering and Architecture, Zhejiang University, Hangzhou 310058, China
[2]Alibaba-Zhejiang University Joint Research Institute of Frontier Technologies, Hangzhou 311121, China
[3]ZhongYuan Institute, Zhejiang University, Zhengzhou 450001, China

Corresponding author: Dianhai Wang (wangdianhai@zju.edu.cn)

This work was supported in part by the National Natural Science Foundation of China under Grant 61773338 and Grant 52072340, and in part by the National Key Research and Development Program of China under Grant 2019YFB1600303.

ABSTRACT Signal coordination plays an important role in urban traffic control systems. Studying the influence of some factors such as the link length on the potential benefits of signal coordination can result in more efficient traffic control. Researchers have observed a highly fluctuating or damped sine-wave type relationship between the link length and the delay in two-way coordinated control, but a clear explanation of this relationship is still lacking. This paper presents a thorough analysis of the mechanism by which link length affects the delay in two-way coordination. The impact of the link length involves two aspects. We first derived formulas for the delay using shockwave queuing profiles that included the impact of the offsets in the two directions. We then conducted numerical experiments employing Robertson's platoon dispersion model to incorporate the impact of platoon dispersion. By comparing the results from the derived formulas and the numerical experiments, we concluded that the periodicity is due to the mutual relation between the offsets in the two directions, whereas the attenuation is due to platoon dispersion. The findings should provide valuable insights for developing a more reasonable correlation degree model for the coordination of adjacent intersections. In addition, we found that platoon dispersion has a negligible influence on the critical link lengths at which the delay cannot be reduced by signal coordination. This means that whether or not platoon dispersion is considered, it will not affect the choice between the simultaneous and the alternative progressions to minimize the delay under a given link length, which is very meaningful in practical work.

INDEX TERMS Control delay, link length, offset, platoon dispersion, two-way coordination.

I. INTRODUCTION

Signal coordination plays an important role in today's urban traffic control systems. It has been widely used to facilitate progressive movements along streets to reduce stops, delays, and fuel consumption [1]. For signal coordination in a large-scale urban street network, it is essential to partition the network into several subareas to achieve better flexibility and efficiency. The premise of subarea partitioning is to identify whether the coordination of adjacent signals will result in better performance than isolated operations [2]. Researchers have found that a number of factors, including the link length, traffic volume, and pre-existing signal timing plan, have significant impacts on the possible benefits of signal coordination [3]. Studying these impacts is helpful for developing more reasonable correlation degree models for the coordination of adjacent intersections and operating more efficient traffic control. In this paper, we focus on the link length's impact on the delay in two-way signal coordination.

The link length's impact on the delay in signal coordination is closely associated with platoon dispersion. When a platoon of vehicles departs from an upstream signal and progresses downstream, it tends to disperse to some extent. The longer the link length is, the greater the dispersion. The purpose of signal coordination is to allow the upstream discharged vehicles to pass the downstream intersection with as little stopping as possible during the green period. Considering traffic flow in one direction, as the amount of dispersion increases, the proportion of vehicles that can pass during the limited green period gradually decreases, resulting in a gradual decline in the benefits of signal coordination [4]. When the platoon disperses to a specific extent, there is no longer a significant difference between coordinated control and isolated control. Therefore, the existence

The associate editor coordinating the review of this manuscript and approving it for publication was Mohamad Afendee Mohamed.

of a critical length between adjacent intersections for signal coordination is usually considered in engineering practice. Researchers have developed various correlation indices for the interconnection of adjacent intersections [5]–[7], and these indices decrease with increasing link length. When the index is greater than a predefined threshold, adjacent intersections should be coordinated. It should be pointed out that these types of correlation indices are all based on one-way coordination scenarios.

For two-way conditions, signal coordination involves progressions in both directions of the link. The sum of the offsets in two directions must be equal to an integer number of the cycle length. When the maximum ratio of vehicles in one direction can pass the green light without stopping, the arrival flow in the other direction may not necessarily be at its maximum ratio for passing the green light [8]. Only under a certain link length can the offset settings achieve the maximum ratio of vehicles arriving to a green light in both directions. For example, when the link length divided by the running speed is exactly equal to half of the cycle length, implementing a two-way alternate progression can achieve the maximum bandwidth of the green waves. When the link length is slightly less than or greater than this specific length, the bandwidth shows a decreasing trend. Under the combined effects of this phenomenon and platoon dispersion, the link length's impact on the delay in two-way coordination becomes rather complicated.

Hu *et al.* [9], Zhou *et al.* [10] and Wen *et al.* [11] proposed similar correlation degree models when studying the subarea partition problem. The unidirectional correlation degree from intersection a to intersection b, $I_{a\to b}$, was expressed as a decreasing function of the link length. They took the greatest correlation degree of the two directions as the two-way coordination correlation degree; that is, $I_{ab} = \max(I_{a\to b}, I_{b\to a})$. In other words, as long as one direction reaches the threshold, two-way coordination should be performed. Because the inherent relationship between the offsets of the two directions is ignored, this approach is computationally efficient but has limited accuracy.

Bie *et al.* [12] derived a function of the arrival flow profile at the downstream intersection for a given link length based on Robertson's platoon dispersion model. Taking 40% of vehicles that arrive during green as a critical condition, they developed methods to calculate the critical length for both one-way and two-way coordination. In numerical examples, the critical lengths for one-way coordination were 1245 m and 1137 m, whereas that for two-way coordination was 613 m. It can be seen that achieving benefits from implementing two-way coordination has stricter requirements for intersection spacing.

Due to the complexity of delay calculations when considering platoon dispersion and offset optimization, simulations and numerical experiments have been used in related research to study the relationship between the link length and the delay reduction from implementing two-way coordination. Chang and Messer [6] conducted a simulation experiment with the PASSER II and TRANSYT-7F software programs and found a highly fluctuating or damped sine-wave type relationship between the link length and control delay. Bie *et al.* [13] studied the influence of link length on the delay in two-way coordination using numerical experiments. They found that the control benefit does not gradually decrease with link length and that there is a curvilinear relationship between link length and control benefit. They used a multivariate regression method to fit the functional relationship. From another perspective, Nie *et al.* [14] studied the influence of changing progression speed on the average delay under a constant link length using VISSIM simulation. The results showed a nonmonotonic relationship between the progression speed and the average delay. Since the link running time equals the ratio of the link length to the progression speed, the nonmonotonic relationship may have causes similar to those of the above two studies. However, neither of these studies provided a detailed explanation of the mechanism by which the delay in two-way coordination is affected.

This paper is intended to provide a thorough analysis of the link length's impact on the delay in two-way coordination. Platoon dispersion plays an important role in the link length's impact. The classic models that describe the platoon's behavior in the literature include Lighthill and Witham's kinematic wave theory, Pacey's diffusion model, and Robertson's recursive model [15]. Lighthill and Witham [16] used a shockwave to describe the transition between two traffic states on a road section that results in no dispersion when predicting downstream arrivals. In Pacey's and Robertson's models [17], [18], dispersions are modeled by assuming specific travel time or speed distributions for vehicles in the platoon.

The rest of this paper is organized as follows. In section 2, we ignored the platoon dispersion's impact to simplify the analysis. We used the shockwave queuing profile to study the spatiotemporal vehicle dynamics from entering to leaving a given link and calculated the delay incurred at the downstream intersection. In section 3, we employed Robertson's model to incorporate the impact of platoon dispersion. We used numerical experiments to calculate the coordination control delays under various link lengths. In section 4, we compared the relationships between link length and control delay with and without considering platoon dispersion. In the last section, we drew conclusions and provided recommendations for future research.

II. THEORETICAL DERIVATION IGNORING THE DISPERSION'S IMPACT

The shockwave queuing profile, also called a time-space diagram, shows the position of each vehicle in time and space as it travels down the street and is delayed by the downstream signal, as shown in the lower part of Fig. 1. Vehicles leave the upstream intersection at speed v when the light turns green. Vehicle c_1 passes through the downstream intersection directly during the green period, whereas vehicle c_2 encounters the red light and stops and waits. The vehicles arriving afterward stop at the end of the queue, and the

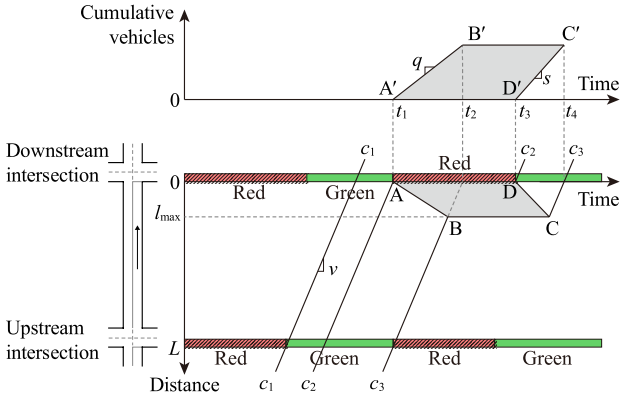

FIGURE 1. Time-space diagram and cumulative plot for vehicles traveling from upstream to downstream.

queuing shockwave formed in this process propagates along the straight line $\overline{AB}$ until it meets vehicle c_3. The shaded region ABCD represents the blocked state of traffic flow. When the downstream light turns green again, vehicle c_2 and its followers start and leave the intersection. The formed discharge shockwave propagates along the straight line $\overline{DC}$ until it encounters vehicle c_3. The length of line $\overline{BC}$ represents the delay of vehicle c_3. Let $l_{\max}$ denote the distance from point B or C to the downstream stop line and k_{jam} denote the jam density. Then, the maximum number of queued vehicles can be calculated as $N = l_{\max}k_{\text{jam}}$. The total vehicle delay is equal to the area of the shaded region ABCD times the jam density, namely, $D = S_{\text{ABCD}}k_{\text{jam}}$.

Although the time-space diagram intuitively depicts the process of queue generation and dissipation, the delay calculation is slightly complicated. Cumulative plots provide a simple method for delay calculation. As shown in the upper part of Fig. 1, when the red light turns on at time t_1, the queue starts to accumulate at the arrival flow rate q. The arrival rate from t_2 to t_3 is zero, and the queue length remains unchanged. At time t_3, the light turns green, and the queue starts to dissipate at the saturation flow rate s. At time t_4, the queue completely clears, and the arriving vehicles directly pass through the intersection during the subsequent green period. The area of the shaded region A′B′C′D′ represents the total delay in one cycle; namely, $D = S_{\text{A′B′C′D′}}$. The delays calculated by the time-space diagram and the cumulative plot have been proven to be equal [19]. Since $S_{\text{A′B′C′D′}}$ is easier to calculate, we used the cumulative plot for delay calculation.

This paper focuses on the link length's impact on the delay in two-way coordination. Therefore, the consideration of other influencing factors, such as the cycle length, traffic volume, and turning ratio, was simplified as much as possible. It appears advantageous to gradually attack the problem. If we try to do too much at once, the algebra becomes so heavy that one may get lost in the details. We assumed that 1) the arrival flow rate and turning ratio for each approach of the two adjacent intersections are symmetric and assigned identical values; 2) the signals operate in a fixed-time mode and are

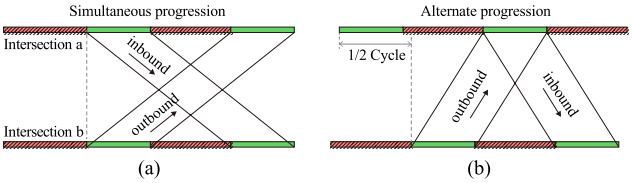

FIGURE 2. Illustration of the two types of progression. (a) Simultaneous progression. (b) Alternate progression.

predetermined based on an ideal signal cycle length and the "equalization of flow ratios" principle; thus, the upstream and downstream intersections have identical cycle length and splits; 3) the platoons are approaching at the same speed in each direction. Under this circumstance, implementing a simultaneous progression or an alternate progression can yield maximal equal bandwidths [20]. As shown in Fig. 2, signals with simultaneous progression simultaneously display the same indication, whereas the alternate offset equals 1/2 cycle. The traffic flow in the two directions is symmetrical, so we calculated the average delay in one direction to represent the overall average delay.

The existence of turning traffic complicates traffic conflicts and phase design at intersections. To facilitate the analysis, we first analyzed the situation where there were only through movements. We then investigated the case where the intersection operated a four-phase signal plan with turning movements. Although the former situation does not exist in reality, it is useful for understanding the nature of the problem and drawing some general conclusions.

A. WITH ONLY THROUGH MOVEMENTS INVOLVED

In the case of only through movements involved, there is no turning flow, and the intersection will perform a two-phase signal plan. We shall separately discuss the situations of simultaneous progression and alternate progression.

When simultaneous progression is performed, the coordinated phases of the upstream and downstream intersections simultaneously turn green. Fig. 3 depicts two different situations where vehicles released during the upstream green period travel downstream and pass the downstream intersection. If vehicles are not blocked by the signal, the running time t_R from upstream to downstream is

$$t_R = \frac{L}{v} \tag{1}$$

where L is the link length (m), and v is the approaching speed (m/s).

Let g be the effective green time and C be the cycle length. When $0 < t_R < g$, as shown in Fig. 3(a), the first half of the platoon encounters the downstream green light and directly passes through the intersection, whereas the second half is blocked by the red light and waits to pass through the intersection until the next cycle. When $g < t_R < C$, as shown in Fig. 3(b), the whole platoon encounters the red light at the downstream intersection, waits for the light to turn green, and then passes the stop line. In the upper part of Fig. 3(a)

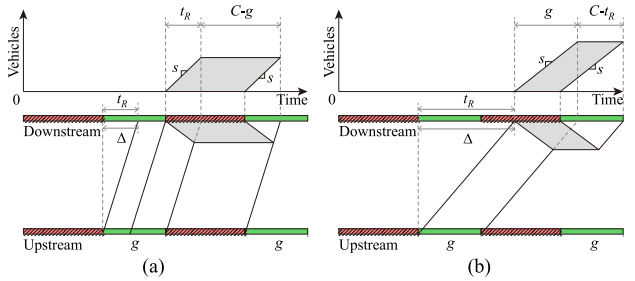

FIGURE 3. Queuing profiles for simultaneous progression with only movements involved. (a) $0 < t_R < g$. (b) $g < t_R < C$.

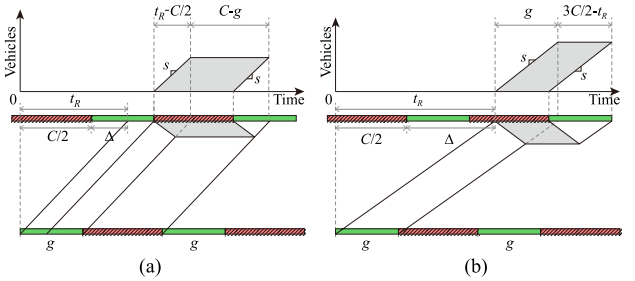

FIGURE 4. Queuing profiles for the alternate progression with only through movements involved. (a) $C/2 < t_R < C/2 + g$. (b) $C/2 + g < t_R < 3C/2$.

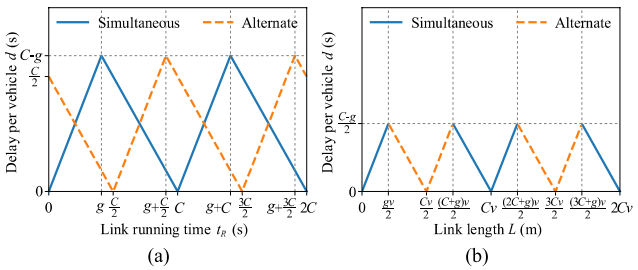

FIGURE 5. Delay when only through movements are involved. (a) Relationship between the average delay and link running time with two types of progression. (b) Relationship between the average delay and link length with the preferred type of progression.

and Fig. 3(b), the shaded area is the total delay in one cycle. The total delay divided by the number of vehicles passing through during green equals the average delay per vehicle. We separately calculated the average delay values d in the two situations, as given by

$$d = \begin{cases} \dfrac{C-g}{g} t_R, & 0 < t_R < g \\ C - t_R, & g < t_R < C \end{cases} \tag{2}$$

When the running time increases by an integer number of cycle lengths, the process of the platoon being delayed at the downstream intersection is unchanged. Therefore, when $t_R > C$, the average delay per vehicle equals that when the running time is equal to mod (t_R, C), and II-B can be rewritten as

$$d = \begin{cases} \dfrac{C-g}{g} \Delta, & \Delta \in [0\ ,\ g) \\ C - \Delta, & \Delta \in [g\ ,\ C) \end{cases} \tag{3}$$

where $\Delta = \text{mod}\,(t_R, C)$ indicates the remainder after t_R is divided by C. In Fig. 3, Δ is the time interval between the arrival of the first vehicle in the platoon and the most recent start of the previous green light.

When the alternate progression is performed, the upstream and downstream coordinated phases differ in the start time by $C/2$. There are also two different situations in which vehicles travel from upstream to downstream, as shown in Fig. 4. Calculating the shaded area in the upper part of Fig. 4 and dividing it by the number of vehicles passing in one cycle, we obtained the average delay per vehicle for the alternate progression as

$$d = \begin{cases} \dfrac{C-g}{g} \left(t_R - \dfrac{C}{2} \right), & t_R \in \left[\dfrac{C}{2}\ ,\ \dfrac{C}{2} + g \right) \\ \dfrac{3C}{2} - t_R, & t_R \in \left[\dfrac{C}{2} + g\ ,\ \dfrac{3C}{2} \right) \end{cases} \tag{4}$$

Considering the complete value range of t_R, the average delay can be expressed as

$$d = \begin{cases} \dfrac{C-g}{g} \Delta, & \Delta \in [0\ ,\ g) \\ C - \Delta, & \Delta \in [g\ ,\ C) \end{cases} \tag{5}$$

where

$$\Delta = \text{mod}\left(t_R - \frac{C}{2}, C \right) \tag{6}$$

As we can see, in Fig. 4, Δ means the time interval between the arrival of the first vehicle in the platoon and the most recent start of the previous green light.

Simultaneous progression and alternate progression are applicable in different conditions. Fig. 5(a) shows the relationship between the average delay and the running time. We see that the curve of the alternate progression is equivalent to the curve of the simultaneous progression moved $C/2$ to the right. In fact, the difference between these two progression types is that their offsets differ by $C/2$.

In practice, the progression with less delay should be selected as the preferred one, as shown in Fig. 5(b). When the link length is $(0, gv/2)$, the simultaneous progression performs better. In this case, the average delay increases with link length. When the link length is $(gv/2, (C+g)v/2)$, the alternate progression operates better. In this case, as the link length increases, the average delay first decreases and then increases. When the link length is $((C+g)v/2, (2C+g)v/2)$, the simultaneous progression performs better. In this case, as the link length increases, the average delay first decreases and then increases. When the link length continues to increase, the delay curve presents periodic fluctuations. Thus, the link length's impact is not monotonous. Moreover, under certain link lengths such as $Cv/2$, Cv, and $3Cv/2$, the average delay achieves the minimum value, whereas under other certain link lengths such as $gv/2$, $(C+g)v/2$, and $(2C+g)v/2$, no matter which progression type is used, the average delay reaches the maximum value. It should be noted that these regularities are useful in

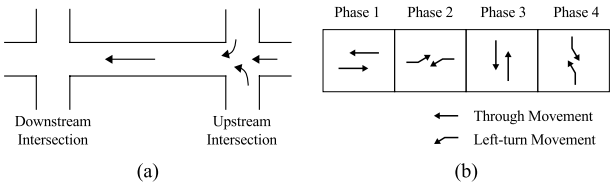

FIGURE 6. (a) Downstream arrivals from the upstream intersection. (b) A typical four-phase signal operation.

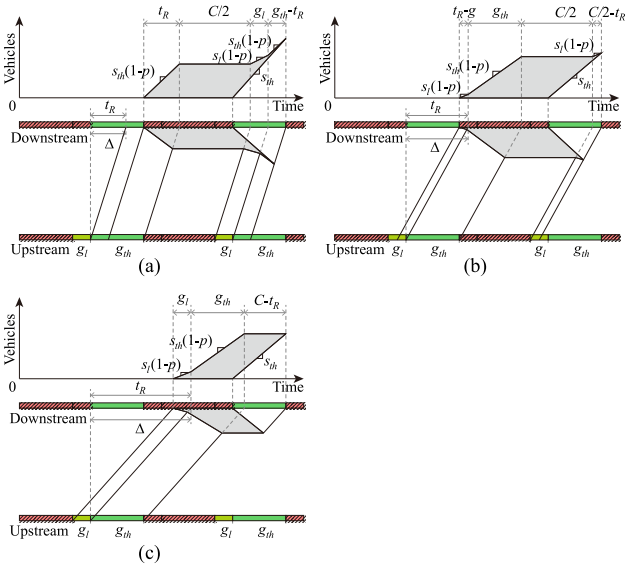

FIGURE 7. Queuing profiles for the simultaneous progression with four-phase signal control. (a) $0 < t_R \le g_{th}$. (b) $g_{th} < t_R \le g_{th} + g_l$. (c) $g_{th} + g_l < t_R \le C$.

the fixed-time control condition, i.e., the cycle length and splits are fixed in duration.

B. FOUR-PHASE SIGNAL CONTROL

Four-phase signal control has broad applications in urban intersections. Fig. 6 shows the downstream arrivals and a typical phase sequence. The downstream arrivals comprise flows from the left-turn, through, and right-turn movements at the upstream intersection. Since right-turn movements are not controlled by the signal and the flow rates are generally low, the right-turn delay can be ignored. Thus, we considered only the through and left-turn movements in the calculation of the delay at intersections.

Let s_{th} and s_l denote the saturation flow rate for the through movement and left-turn movement, respectively. Let g_{th} and g_l be the effective green time for the through and left-turn movements, respectively, and let p be the left-turn ratio for the downstream arrivals with right-turn vehicles excluded. Then, the through ratio equals $1 - p$. Fig. 7(a) shows the queuing profiles for the downstream through movement under the simultaneous progression with $0 < t_R \le g_{th}$. The arrival flow rate at the downstream intersection is piecewise. During the t_R period after the downstream red light turns on, the flow comes from the upstream through movement, and the flow rate is $s_{th}(1-p)$. One-half cycle later, vehicles from the upstream left-turn movement arrive, the flow rate is $s_l(1-p)$, and the duration is g_l. Then, vehicles from the upstream through movement arrive at a flow rate of $s_{th}(1-p)$, and the duration is $g - t_R$. When the green light turns on, the queue begins to dissipate at the saturation flow rate s_{th}. It clears exactly when the signal turns red again.

When t_R continues to increase, the queuing profiles in the cases of $g_{th} < t_R \le C/2$ and $C/2 < t_R \le C$ are shown in Fig. 7(b) and Fig. 7(c), respectively. Combining these three situations and using the method mentioned earlier, we calculated the average delay of the through movement as

$$d_{th} = \begin{cases} \left[\dfrac{(1-p)\,C}{g_{th}} - 1\right]\Delta + \dfrac{pC}{4}, & \text{if } \Delta \in [0, g_{th}), \\ \left(\dfrac{pC}{g_l} - 1\right)\left(\Delta - \dfrac{C}{2}\right) & \\ \quad + \dfrac{pC}{4} + \dfrac{C}{2}, & \text{if } \Delta \in \left[g_{th}, \dfrac{C}{2}\right), \\ -\Delta + \dfrac{pC}{4} + C, & \text{if } \Delta \in \left[\dfrac{C}{2}, C\right). \end{cases} \tag{7}$$

where

$$\Delta = \mathrm{mod}\,(t_R, C) \tag{8}$$

In (8), Δ is the time interval between the arrival of the first vehicle in the platoon from the upstream through phase and the most recent start of the green light for the downstream through phase.

For the downstream left-turn movement, the analysis method is similar to that of the through movement. The average delay is given as

$$d_l = \begin{cases} \left[\dfrac{(1-p)\,C}{g_{th}} - 1\right]\Delta & \\ \quad - \dfrac{(1-p)\,C}{4} + g_{th}, & \text{if } \Delta \in [0, g_{th}), \\ \left(\dfrac{pC}{g_l} - 1\right)(\Delta - g_{th}) & \\ \quad + \dfrac{3\,(1-p)\,C}{4}, & \text{if } \Delta \in \left[g_{th}, \dfrac{C}{2}\right), \\ -\Delta + \dfrac{pC}{4} + \dfrac{3C}{4} + g_{th}, & \text{if } \Delta \in \left[\dfrac{C}{2}, C\right). \end{cases} \tag{9}$$

where

$$\Delta = \mathrm{mod}\,(t_R - g_l, C) \tag{10}$$

In (10), Δ is the time interval between the arrival of the first vehicle in the platoon from the upstream left-turn phase and the most recent start of the green light for the downstream through phase.

Considering both through and left-turn movements, the average delay per vehicle under the simultaneous progression is

$$d = \frac{g_{th} s_{th} d_{th} + g_l s_l d_l}{g_{th} s_{th} + g_l s_l} = (1-p)\,d_{th} + p d_l \tag{11}$$

We obtained the average delay per vehicle under the alternate progression in a similar way. The delay curve is still

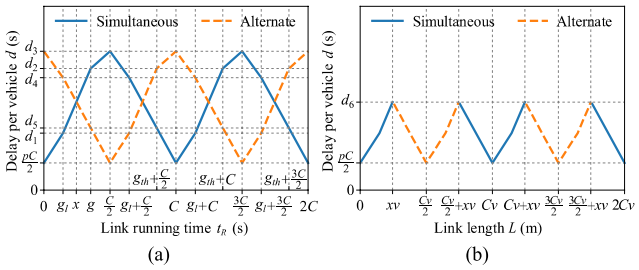

FIGURE 8. Delay when a four-phase signal operation is considered. (a) Relationship between the average delay and the link running time with two types of progression. (b) Relationship between the average delay and the link length with the preferred type of progression.

equivalent to the curve of the simultaneous progression shifting $C/2$ to the right, as shown in Fig. 8(a). We select the progression type with less delay as the preferred one, as shown in Fig. 8(b). In Fig. 8(a), the curves corresponding to the two progression types cross at $t_R = x$, where x should satisfy $0 < x < C/2$. It can be further proven that $g_l < x < g_{th}$ under certain conditions satisfying $s_{th}/s_l \leq 3$ and $p < 0.21$(see the Appendix). Solving x yields $x = pg_l + g_{th}/[2(1-p)]$. Under such conditions, the average delay for the preferred progression type is given as

$$d = \begin{cases} \left[\dfrac{(1-p)^2 C}{g_{th}} - 1\right]\Delta + \dfrac{pC}{2}, & \text{if } \Delta \in [0, g_l), \\ \left[\dfrac{(1-p) C}{g_{th}} - 1\right]\Delta + \dfrac{pC}{2} & \\ \quad - \dfrac{p(1-p) C g_l}{g_{th}}, & \text{if } \Delta \in [g_l, x), \\ -\Delta + \dfrac{pC}{2} + \dfrac{C}{2}, & \text{if } \Delta \in \left[x, \dfrac{C}{2}\right). \end{cases} \tag{12}$$

where

$$\Delta = \mathrm{mod}\left(t_R, \frac{C}{2}\right) \tag{13}$$

As shown in Fig. 8(b), the simultaneous progression performs better when the link length is $(0, xv)$. In this case, the average delay increases with the link length. When the link length is $(xv, Cv/2 + xv)$, the alternate progression operates better. In this case, as the link length increases, the average delay first decreases and then increases. When the link length is $(Cv/2 + xv, Cv + xv)$, the simultaneous progression performs better. Again, in this case, as the link length increases, the average delay first decreases and then increases. As the link length continues to increase, the delay curve presents periodic fluctuations. The link length's impact is not monotonous. When the link length is within a certain interval, the simultaneous progression operates better, whereas in the next interval, the alternate progression operates better; then, in the next interval, the simultaneous progression operates better again; the two modes alternate. Moreover, under certain link lengths such as $Cv/2$, Cv, and $3Cv/2$, the average delay achieves the minimum value, whereas under other certain link lengths such as xv, $Cv/2+xv$, and $Cv+xv$, regardless of which progression type is used, the average delay reaches the maximum value. These regularities are similar to the case where only through movements are involved.

III. NUMERICAL EXPERIMENTS BASED ON ROBERTSON'S PLATOON DISPERSION MODEL

The model formulated in the previous section is based on the premise that the platoon dispersion's impact can be ignored, but the dispersion has an effect in reality. Because Robertson's model rationally represents platoon dispersion and is easy to calculate, it has been adopted in a number of signal optimization and control systems, such as TRANSYT [18], SCOOT [21], and SATURN [22], to estimate the downstream arrival flow profile. On the other hand, Seddon [23], [24] and Wang *et al.* [25] reported that the form of the platoon dispersion model has no significant influence on the accuracy of the delay calculation. Therefore, in this section, based on Robertson's platoon dispersion model, we used numerical experiments to incorporate the influence of dispersion on the delay in two-way coordination.

With a given discharge flow profile, Robertson's model can be used to estimate the arrival flow rate at the downstream stop line at any time t. The formula is as follows:

$$q'_t = Fq_{t-T} + (1-F)q'_{t-1} \tag{14}$$

with

$$F = \frac{1}{1+\alpha T} \tag{15}$$

where q'_t is the estimated arrival flow at the downstream intersection in time step t, F is the dimensionless smoothing factor, q_{t-T} is the departure flow at the upstream intersection in time step $t-T$, α is the dimensionless platoon dispersion factor, $T = \beta t_a$ is the platoon arrival time, t_a is the average running time on the link, and β is a dimensionless adjustment factor. Before this model is applied, its parameters, α and β, require proper calibration to represent the dispersion under actual traffic conditions. We adopted a frequently used method (see [26] and [27]) for calibration. α is increased from 0 to 1 in increments of 0.01, while β is held constant at 0.8. The goal is to find an optimal α that minimizes the sum of the squared errors between observed and estimated downstream arrivals:

$$\phi(\alpha) = \sum_{t=1}^{m} \left(q''_t - q'_t\right)^2 \tag{16}$$

where q''_t is the observed arrival flow rate at the downstream location in time step t, and m is the number of time steps. We used a time step of 1 s/step.

To cover various traffic conditions, we selected 7 study sites in Hangzhou and Guiyang in China for calibration. Data were collected by automatic number-plate recognition (ANPR) systems. Each study site had three cameras installed at the upstream stop lines and one camera placed in the middle of the link. These cameras recognized a vehicle's

TABLE 1. Summary of the Study Sites and Data Collected.

Site	Number of lanes	Distance (m)	Number of platoons	Maximum platoon size (veh)	Average platoon size (veh)	Average travel speed (m/s)
A	2	240	73	27	13.08	11.03
B	2	392	66	24	11.90	10.76
C	3	354	96	47	28.50	12.58
D	3	565	125	32	15.54	9.00
E	3	819	86	46	24.93	11.52
F	4	203	110	57	26.97	10.40
G	4	425	65	33	12.44	12.57

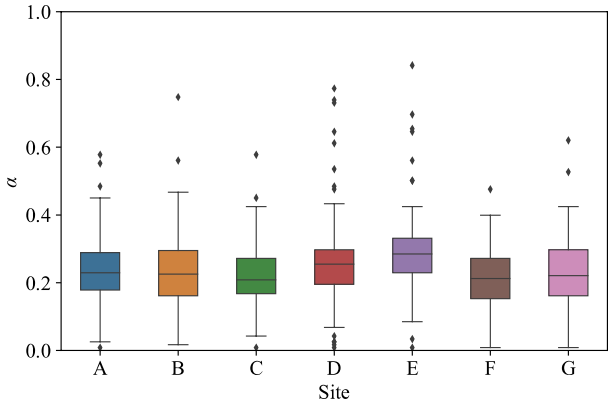

FIGURE 9. Distribution characteristics of the calibrated α at each study site.

TABLE 2. Summary Statistics of the Calibrated α at Each Study Site.

Site	α average	α standard deviation
A	0.24	0.11
B	0.24	0.12
C	0.22	0.10
D	0.26	0.13
E	0.30	0.13
F	0.21	0.09
G	0.23	0.11

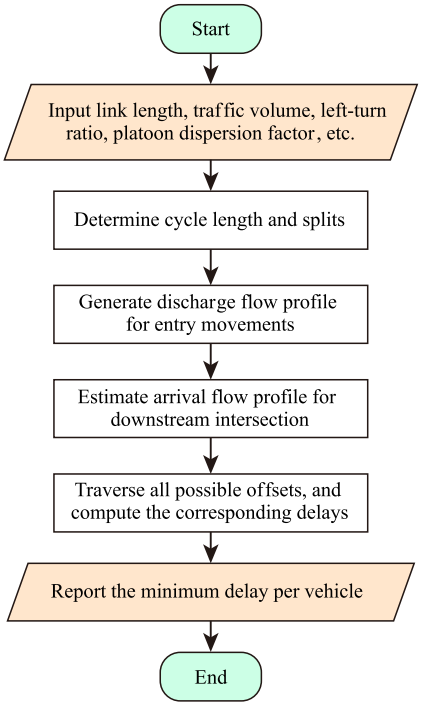

FIGURE 10. Procedures for calculating the optimal delay in the numerical experiments.

license plate and recorded the license plate number, timestamp, lane number, and other information when the vehicle passed through the detection section. We used the ANPR data during and after peak hours in April and May 2019 to cover different traffic conditions. The data at each study site include two 2-hour periods. The number of lanes ranges from 2 to 4, and the link length ranges from 203 m to 819 m. We introduced the data cleaning method proposed in [28] to remove noise from the data and match the license plate numbers at different detection points. After data cleaning, two adjacent vehicles with a headway less than 4 s were considered to belong to the same platoon. A summary of the obtained data is listed in Table 1.

Fig. 9 depicts the distribution of the calibrated α of the 7 study sites. Each calibrated value is represented by a small dot. The majority (85.20%) of the calibrated α values are concentrated in the interval of 0.1 to 0.4. Table 2 lists the mean and standard deviation of α. To study the influence of the link length under different amounts of dispersion, we took 0.15, 0.25, and 0.35 as representative values.

We used the procedures shown in Fig. 10 to obtain the coordinated control delays under different link lengths. First, we calculated the cycle length and splits at intersections. According to the "equalization of flow ratios" principle, the green time is allocated among the various signal phases in proportion to the flow ratio for each phase. The cycle length is calculated by $C = L_c / \left(1 - \sum y_i\right)$, where L_c is the cycle lost time, and y_i is the flow ratio for phase i and equal to the ratio of the arrival flow rate to the saturation flow rate. For phase i, the green time g_i is computed by $g_i = (C - L_c)\, y_i / \sum y_i + l_i$, where l_i is the phase lost time. The cycle length and splits have a precision of 1 s. Then, we used Robertson's model to estimate the downstream arrival flow profiles corresponding to the upstream discharge flow profiles. The precision of the arrivals per time step is 0.0001 veh. Finally, we traversed all possible offsets and determined the minimum delay at the downstream intersection.

In the numerical experiments, we set the link length within the range of 100 to 1000 m. Each intersection approach had one exclusive left-turn lane and two through lanes. With no loss of generality, we used 1400 veh/h and 1600 veh/h as their saturated flow rates, respectively. The lost time per phase was

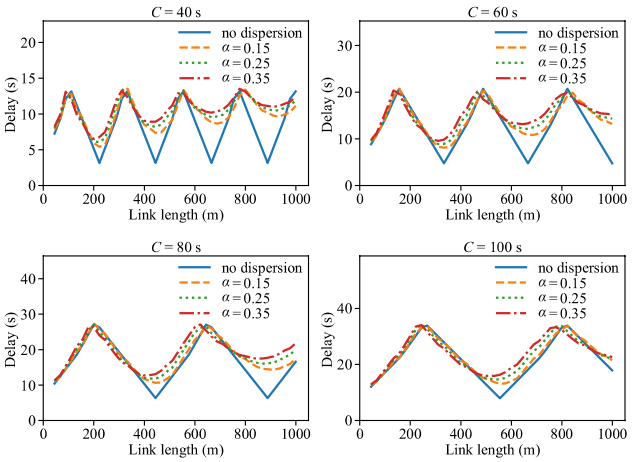

FIGURE 11. The delay in two-way coordination with respect to the link length under various cycle lengths.

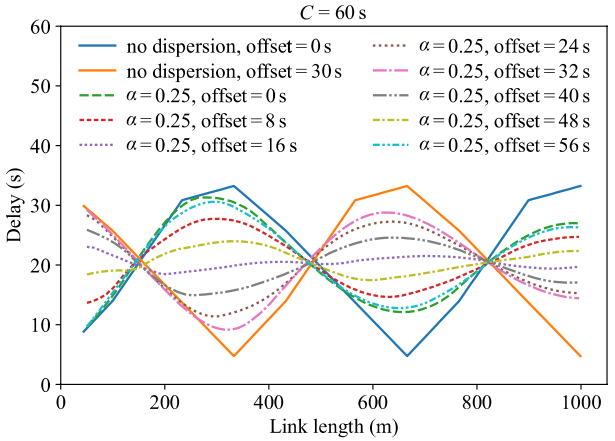

FIGURE 12. Delay with respect to the link length with various offsets.

4 s, and the total lost time per cycle was 16 s. To obtain results under different traffic loadings, we took 800, 980, 1070, and 1120 veh/h as the average flow rates on the link. With a left-turn ratio of 15%, the corresponding signal cycle lengths were 40, 60, 80, and 100 s.

IV. RESULTS AND DISCUSSION

Apart from the numerical experiment results, we calculated the delays with no dispersion considered using the formulas derived in section 2 for comparison. Fig. 11 depicts the relationship between link length and the delay in two-way coordination under various traffic loadings. The corresponding cycle lengths are 1) $C = 40$ s, 2) $C = 60$ s, 3) $C = 80$ s, and 4) $C = 100$ s. In each subfigure, we plotted curves under three different platoon dispersion factors (shown as dashed lines) and under no dispersion (indicated by the solid line). The delay increases and decreases periodically as the link length increases regardless of whether the dispersion's impact is considered. When the dispersion's impact is not involved, the local extremums of the delay are stable. When the impact is involved, as the link length increases, the local maximum does not change, whereas the local minimum gradually increases, and the curve's volatility decreases. This is because the arrivals spread out over a longer period as the rate of dispersion increases, and thereby, the benefit of coordinated control decreases. When the link length is sufficiently long, the arrivals would be approximately uniform, the coordination would provide little benefit, and the curve would converge to the maximum delay. In addition, the greater α is, the greater the rate of dispersion, and the faster the curve converges.

According to the regularities unveiled from the formulas, we know that the local maximum in Fig. 11 indicates that the delay cannot be further reduced regardless of whether simultaneous progression or alternate progression is performed. Taking a cycle length of 60 s as an example, we plotted in Fig. 12 the delay of coordinated control with various offsets. The aforementioned local maximum occurs at a critical point where the delay cannot be reduced by changing the offset. When the link length is far from the critical point, implementing an appropriate progression can achieve the optimal delay.

In each subfigure of Fig. 11, the fluctuation cycles of the curves are approximately equivalent regardless of the dispersion's impact. Comparing subfigures under different cycle lengths, we see that the fluctuation cycle is proportional to the cycle length. According to (12) and III, the fluctuation cycle is equal to $Cv/2$. When carefully examining the critical link lengths corresponding to the local maxima, we still see subtle differences. Comparing the dashed curves, we see that when the value of α is greater, the fluctuation cycle is smaller; that is, the n^{th} local maximum or local minimum occurs at a shorter link length. This is because Robertson's model assumes that the first vehicle's arrival time is equal to the average travel time times 0.8. The greater α is, the greater the rate of dispersion, leading to a longer average travel time and a lower average travel speed. Recognizing that the fluctuation cycle is proportional to the travel speed, this phenomenon can be explained. Table 3 shows the summary statistics of the critical points from the derived formulas and the numerical experiments.

Comparing the curves from the derived formulas and numerical experiments, we find that the platoon dispersion's impact on the delay in two-way coordination is closely related to the link length and cycle length. When the link length is near each critical point that corresponds to a local minimum, the dispersion has the most obvious impact on the delay. We characterized the degree of the dispersion's impact as $\theta = (d' - d)/d_{\max}$, where d' is the delay estimated from the numerical experiment and d and $d_{\max}$ are the delay and the maximum delay calculated by the derived formulas, respectively. Fig. 13 shows the impact degrees under different traffic loadings and dispersion rates. According to a recent report published by MoHURD [29], most of China's major cities have an average intersection spacing within the range of 200-600 m. Cities in some developed

TABLE 3. Summary Statistics of the Critical Link Length Corresponding to the Local Maximum Delay.

		Average (m)	Standard deviation (m)	Range (m)
$C = 40$ s	1st CL	101	3.83	8
	2nd CL	319	6.83	16
	3rd CL	548	8.33	20
	4th CL	786	11.78	28
$C = 60$ s	1st CL	149	6.00	12
	2nd CL	477	11.49	24
	3rd CL	824	11.55	28
$C = 80$ s	1st CL	199	9.45	20
	2nd CL	637	17.09	36
$C = 100$ s	1st CL	248	12.00	24
	2nd CL	796	22.98	48

CL denotes the critical link length corresponding to the local maximum delay.

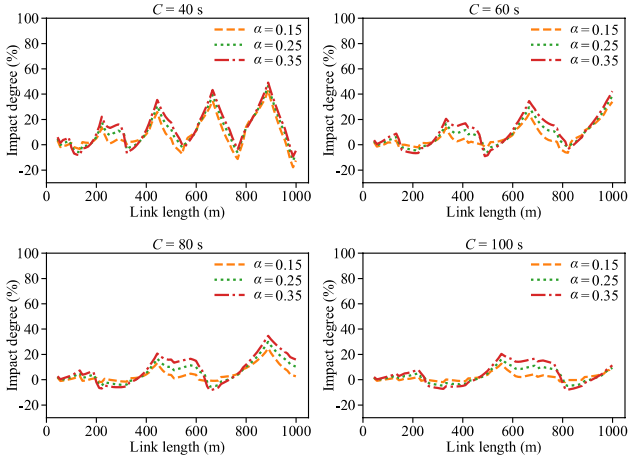

FIGURE 13. Platoon dispersion's impact degree on the delay with respect to link length under various cycle lengths and dispersion rates.

countries may have a denser road network [30]. In most cases, the cycle length for coordinated control with a four-phase signal plan is greater than 60 s. Under such circumstances, the impact of the dispersion reaches the maximum degree of approximately 22% when the link length equals $Cv/2$. The greater α is, the greater the maximum degree of the dispersion's impact. Moreover, there are no significant differences in the maximum degrees under different cycle lengths.

The left-turn ratio usually has a direct effect on the delay. We analyzed the relationship between the link length and the delay under different left-turn ratios with $C = 80$ s. Fig. 14 shows the results when the left-turn ratios are 5%, 15%, and 30%. Fig. 14(a) shows that a higher left-turn ratio yields a greater delay. However, the critical link lengths corresponding to the curve's local extremums do not change significantly with the left-turn ratio. Fig. 14(b) presents the platoon dispersion's impact on the delay. The greater the

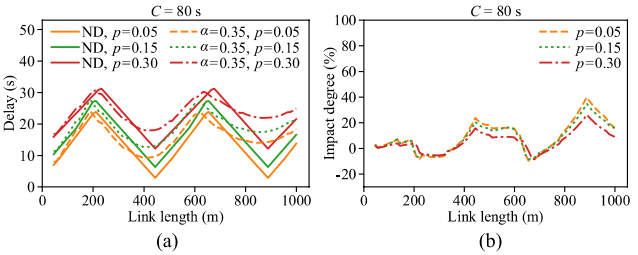

FIGURE 14. (a) The delay in two-way coordination with respect to the link length under different left-turn ratios (ND denotes no dispersion). (b) Platoon dispersion's impact degree with respect to the link length under different left-turn ratios.

left-turn ratio is, the lower the maximum impact degree. This is mainly because the $d_{\max}$ in the denominator of the degree increases with the left-turn ratio, whereas changes in the delay difference (i.e., $d' - d$) are not significant. In the range where link lengths are less than 600 m, the maximum impact degree is approximately 25%.

V. CONCLUSION

This paper aims to reveal the mechanism by which link length affects the delay in two-way signal coordination. The link length's impact involves two areas: the impact of the inherent relationship between the offsets of the two directions and the impact of platoon dispersion. In this paper, we first analyzed the impact of the offsets through theoretical derivation and ignored the dispersion's impact. Then, we investigated the dispersion's impact by comparing the results from the derived formulas with the numerical experiments, which employed Robertson's platoon dispersion model. The analysis leads to the following conclusions:

First, the delay in two-way coordination changes periodically with increasing link length and converges step by step to a state where the benefit of coordinated control is zero. The periodicity is due to the mutual relation between the offsets in the two directions, whereas the attenuation is due to platoon dispersion.

Second, platoon dispersion has a negligible influence on the critical link lengths at which the delay cannot be reduced by optimizing offsets. Therefore, although the derived formulas ignore the dispersion's impact, they can be used to identify whether adjacent intersections should be coordinated, and, if so, which type of progression to use under a given link length.

This paper contributes to the literature in two ways. On the one hand, it provides a clear explanation of the mechanism through which link length impacts the delay in two-way signal coordination. The results can assist in developing a more reasonable correlation degree model for the coordination of adjacent intersections. On the other hand, the findings suggest that the platoon dispersion's impact can be ignored when determining the appropriate progression type to minimize the delay under a given link length, which is very meaningful in practical work.

VI. FUTURE WORKS

Some limitations of our study are worth mentioning, as they provide additional directions for further research. First, we assumed that the intersections operate under symmetric demand. Thus, the signal control scheme was relatively simplified. More general demand flow patterns, for example, asymmetric traffic flows, can be considered in future research. Second, we mostly considered the link length's impact on the delay in our analysis. It would be of significance to consider other performance indicators such as the number of stops and emissions in the future.

APPENDIX

It can be proven that $g_l < x < g_{th}$ when satisfying $s_{th}/s_l \leq 3$ and $p < 0.21$ as follows.

When $t_R = g_l$, the average delays for the simultaneous progression and alternate progression are

$$d_1 = pC/2 - g_l + (1-p)^2 C g_l / g_{th}$$

and

$$d_4 = pC/2 + C/2 - g_l$$

respectively.

When $t_R = g_{th}$, the average delays are

$$d_2 = (1-p)C/2 + g_l - p(1-p)Cg_l/g_{th}$$

and

$$d_5 = pC/2 + g_l$$

Since $g_{th}s_{th}p + g_l s_l p = g_l s_l$, we have $g_l/g_{th} = s_{th}p/[s_l(1-p)]$.

Since $p < 1/2$,

$$d_4 - d_1 = C\left[1/2 - p(1-p)\, s_{th}/s_l\right]$$

and

$$d_2 - d_5 = C\left[1/2 - p - p^2 s_{th}/s_l\right]$$

are monotonically decreasing functions of p and s_{th}/s_l, where s_{th}/s_l roughly equals the ratio of the through lane number to the left-turn lane number.

When $s_{th}/s_l = 3$, $1/2 - p(1-p)\, s_{th}/s_l > 0$ holds for $p < 0.21$, whereas $1/2 - p - p^2 s_{th}/s_l > 0$ holds for $p < 0.27$.

Thus, $d_4 - d_1 > 0$ and $d_2 - d_5 > 0$ are true and thereby $g_l < x < g_{th}$ when satisfying $s_{th}/s_l \leq 3$ and $p < 0.21$.

REFERENCES

[1] S. Ding, X. Chen, L. Yu, and X. Wang, "Arterial offset optimization considering the delay and emission of platoon: A case study in Beijing," *Sustainability*, vol. 11, no. 14, p. 3882, Jul. 2019, doi: 10.3390/su11143882.

[2] R. L. Gordon, P. E. Warren, and P. E. Tighe, "Traffic control systems handbook," Federal Highway Admin., Washington, DC, USA, Tech. Rep. FHWA-HOP-06-006, Oct. 2005. Accessed: Nov. 10, 2020. [Online]. Available: https://ops.fhwa.dot.gov/publications/fhwahop06006/index.htm

[3] Y. Bie, D. Wang, Q. Wei, and D. Ma, "Development of correlation degree model between adjacent signal intersections for subarea partition," in *Proc. 11th Int. Conf. Chin. Transp. Prof. (ICCTP)*, Nanjing, China, Apr. 2012, pp. 1170–1180, doi: 10.1061/41186(421)115.

[4] L. Zhao, L. R. Rilett, and E. Tufuor, "Calibrating the Robertson's platoon dispersion model on a coordinated corridor with advance warning flashers," *Transp. Res. Rec., J. Transp. Res. Board*, vol. 2623, no. 1, pp. 10–18, Jan. 2017, doi: 10.3141/2623-02.

[5] H. N. Yagoda, E. H. Principe, C. E. Vick, and B. Leonard, "Subdivision of signal systems into control areas," *Traffic Eng.*, vol. 43, no. 12, pp. 42–46, Sep. 1973.

[6] E. Chang and C. Messer, "Warrants for interconnection of isolated traffic signals," Texas Transp. Inst., College Station, TX, USA, Tech. Rep. 293-1F, Aug. 1986. Accessed: Nov. 10, 2020. [Online]. Available: https://static.tti.tamu.edu/tti.tamu.edu/documents/293-1F.pdf

[7] H. Lan and X. Wu, "Research on key technology of signal control subarea partition based on correlation degree analysis," *Math. Problems Eng.*, vol. 2020, pp. 1–12, Mar. 2020, doi: 10.1155/2020/1879503.

[8] B. Cesme and P. G. Furth, "Self-organizing traffic signals using secondary extension and dynamic coordination," *Transp. Res. C, Emerg. Technol.*, vol. 48, pp. 1–15, Nov. 2014, doi: 10.1016/j.trc.2014.08.006.

[9] Y. Hu, Y. Wang, J. Zhang, and H. Yu, "Correlation degree analysis of arterial adjacent intersections for coordinated control subunit partition," *Adv. Mech. Eng.*, vol. 10, no. 1, Jan. 2018, Art. no. 1687814017748748, doi: 10.1177/1687814017748748.

[10] Z. Zhou, S. Lin, and Y. Xi, "A fast network partition method for large-scale urban traffic networks," *J. Ctrl. Theory Appl.*, vol. 11, no. 3, pp. 359–366, Aug. 2013, doi: 10.1007/s11768-013-2031-0.

[11] L. Wen, B. Dong, P. Li, and A. Yan, "Signal coordination control based on comprehensive correlation degree," *IOP Conf. Ser., Earth Environ. Sci.*, vol. 638, Feb. 2021, Art. no. 012030, doi: 10.1088/1755-1315/638/1/012030.

[12] Y. Bie, D. Wang, Y. Zhao, and X. Song, "Calculation method of critical coordination link length between two adjacent intersections," *J. Beijing Univ. Technol.*, vol. 39, no. 2, pp. 239–244, 2013.

[13] Y. Bie, D. Wang, and X. Qu, "Modelling correlation degree between two adjacent signalised intersections for dynamic subarea partition," *IET Intell. Transp. Syst.*, vol. 7, no. 1, pp. 28–35, Mar. 2013, doi: 10.1049/iet-its.2011.0224.

[14] C. Nie, J. Shi, and Q. Lin, "Research on reliability of traffic signal coordination control for urban artery," in *Proc. CICTP*, Jul. 2019, pp. 2706–2715, doi: 10.1061/9780784482292.235.

[15] B. Paul, S. Mitra, and B. Maitra, "Calibration of Robertson's platoon dispersion model in non-lane based mixed traffic operation," *Transp. Developing Economies*, vol. 2, no. 2, p. 11, Jun. 2016, doi: 10.1007/s40890-016-0016-7.

[16] M. J. Lighthill and G. B. Whitham, "On kinematic waves II. A theory of traffic flow on long crowded roads," *Proc. Roy. Soc. A, Math., Phys. Eng. Sci.*, vol. 229, no. 1178, pp. 317–345, 1955, doi: 10.1098/rspa.1955.0089.

[17] G. M. Pacey, "The progress of a bunch of vehicles released from a traffic signal," Road Research Laboratory, London, U.K., Tech. Rep. No.Rn/2665/GMP, 1956.

[18] D. I. Robertson, "TRANSYT: A traffic network study tool," Road Res. Lab., Crowthorne, Berkshire, U.K., Tech. Rep. RRL LR 253, 1969.

[19] Y. Liu, J. Guo, and Y. Wang, "Vertical and horizontal queue models for oversaturated signal intersections with quasi-real-time reconstruction of deterministic and shockwave queueing profiles using limited mobile sensing data," *J. Adv. Transp.*, vol. 2018, pp. 1–19, Jun. 2018, doi: 10.1155/2018/6986198.

[20] P. G. Furth, A. T. M. Halawani, J. Li, W. Hu, and B. Cesme, "Using traffic signal control to limit speeding opportunities on bidirectional urban arterials," *Transp. Res. Rec., J. Transp. Res. Board*, vol. 2672, no. 18, pp. 107–116, Dec. 2018, doi: 10.1177/0361198118790638.

[21] P. B. Hunt, D. I. Robertson, R. D. Bretherton, and R. I. Winton, "SCOOT—A traffic responsive method of coordinating signals," Road Res. Lab., Wokingham, U.K., Tech. Rep. RRL Report LR 1041, 1981.

[22] M. D. Hall, D. Vliet, and L. Willumsen, "SATURN-a simulation-assignment model for the evaluation of traffic management schemes," *Traffic Eng. Control*, vol. 21, pp. 168–176, Apr. 1980.

[23] P. A. Seddon, "Another look at platoon dispersion: The diffusion theory," *Traffic Eng. Control*, vol. 13, no. 9, pp. 388–390, 1972.

[24] P. A. Seddon, "Another look at platoon dispersion: The recurrence relationship," *Traffic Eng. Control*, vol. 13, no. 10, pp. 442–444, 1972.

[25] D. Wang, Y. Zhang, and Z. Wang, "Study of platoon dispersion models," in *Proc. 82nd Annu. Meeting Transp. Res. Board*, Washington, DC, USA, Jan. 2003, pp. 3563–3571.

[26] Y. Bie, Z. Liu, D. Ma, and D. Wang, "Calibration of platoon dispersion parameter considering the impact of the number of lanes," *J. Transp. Eng.*, vol. 139, no. 2, pp. 200–207, 2013, doi: 10.1061/(ASCE)TE.1943-5436.0000443.

[27] B. Paul, M. Ramteke, B. Maitra, and S. Mitra, "New approach for calibrating Robertson's platoon dispersion model," *J. Transp. Eng., A, Syst.*, vol. 144, no. 5, May 2018, Art. no. 04018014, doi: 10.1061/JTEPBS.0000141.

[28] E. Kazagli and H. N. Koutsopoulos, "Estimation of arterial travel time from automatic number plate recognition data," *Transp. Res. Rec., J. Transp. Res. Board*, vol. 2391, no. 1, pp. 22–31, Jan. 2013, doi: 10.3141/2391-03.

[29] *Annual Report on Road Network Density in Major Chinese Cities*, Ministry of Housing and Urban-Rural Development, Beijing, China, 2018.

[30] W. Yu, "Assessing the implications of the recent community opening policy on the street centrality in China: A GIS-based method and case study," *Appl. Geography*, vol. 89, pp. 61–76, Dec. 2017, doi: 10.1016/j.apgeog.2017.10.008.

YANLEI CUI received the B.S. degree in urban planning from Zhejiang University, Zhejiang, China, in 2016, where he is currently pursuing the Ph.D. degree majoring in road and transportation engineering. His research interests include the area of traffic control and road network design.

YI YU was born in 1995. She received the B.S. degree in civil engineering from Zhejiang University, Zhejiang, China, in 2017, where she is currently pursuing the Ph.D. degree. Her research interests include traffic flow theories and traffic state identification.

DIANHAI WANG received the Ph.D. degree in transportation engineering from Beijing Jiaotong University, Beijing, China, in 1995.

He is currently a Full Professor with the Institute of Transportation Engineering, College of Civil Engineering and Architecture, Zhejiang University, Hangzhou, China. On these topics, he has published more than 200 articles in related journals, such as *Transportation Research Part—A: Policy and Practice*, *Transportation Research Part—C: Emerging Technologies*, and the *Journal of Urban Planning and Development*. His research interests include traffic control, traffic flow theory, and traffic information. He is a member of China Higher Education Steering Committee, Traffic Engineering Subject, and a member of China City Planning Academic Committee. He received the National Science and Technology Progress Award, in 2004, and the Science and Technology Progress Award of Jilin province, in 2009.